OVERVIEW OF THE CIT PHYSICS DESIGN

G. H. NEILSON[a], D. B. BATCHELOR[a], G. BATEMAN, M. G. BELL, J. BIALEK, B. J. BRAAMS[b], J. N. BROOKS[c], R. J. GOLDSTON, J. R. HAINES[d], D. N. HILL[e], W. A. HOULBERG[a] S. C. JARDIN, C. E. KESSEL, S. S. MEDLEY, F. W. PERKINS, R. D. PILLSBURY[f], N. POMPHREY, M. PORKOLAB[f], W. T. REIERSEN, R. O. SAYER[a], J. E. SCHARER[g], J. A. SCHMIDT, D. J. SIGMAR[f], J. C. SINNIS, R. D. STAMBAUGH[h], D. STOTLER, D. J. STRICKLER[a], M. ULRICKSON, R. E. WALTZ[h], K. M. YOUNG, and J. J. YUGO[a],
Princeton Plasma Physics Laboratory, P.O. Box 451, Princeton, NJ 08543, (609) 243-2726.

ABSTRACT

The Compact Ignition Tokamak is a high-performance device designed to study the physics of burning plasmas. Key physics aspects of the design are described, including plasma performance, disruption handling, power handling, ICRF heating, and diagnostics.

INTRODUCTION

Continued progress in the development of magnetic-confinement fusion energy requires a new facility to study the physics of burning plasmas. The Compact Ignition Tokamak (CIT) is being designed to meet this requirement.[1] Its physics mission is to determine the confinement physics, operational limits, and alpha-particle dynamics of DT-burning plasmas. To accomplish this the facility must produce enough fusion power that the plasma heating from alpha particles will be at least as great as that from auxiliary heating systems (Q=5). This is the minimum performance needed to ensure that potential alpha-driven instabilities, alpha-particle losses, and alpha-related effects on the bulk plasma behavior can be diagnosed and characterized.

PLASMA PERFORMANCE

The major device parameters of the CIT (Table 1) have been chosen such that, even with relatively conservative physics assumptions, the minimum level of performance can be realized. Moreover, the CIT design incorporates features, such as a divertor and low–Z first wall materials, that have been conducive to high performance in existing tokamak experiments. The engineering philosophy follows that pioneered by the Alcator devices in the use of a high magnetic field. Together with the high elongation, this allows very high plasma currents to be imposed while maintaining $q_{95} \geq 3.2$, a regime where existing tokamaks can obtain relatively disruption-free operation.

Minimum-performance projections are depicted in Figure 1. An energy gain Q=5 is obtained with 20 MW of auxil-

Table 1. CIT Device Parameters

Toroidal field, B_T	9 T
Plasma current, I_P	11.8 MA
Flattop pulse length, t_{flat}	10 s
Major radius, R_0	2.59 m
Minor radius, a	0.795 m
Aspect ratio, A	3.3
Safety factor, q_{95}	3.2
Elongation, κ_{95}	2.0
Triangularity, δ_{95}	0.25-0.35
Configurations:	
Divertor	Double and single-null
Limiter	Inboard limiter
Fusion power, P_{fus}	100–500 MW
Alpha power, P_α	20–100 MW
Auxiliary power, P_{aux}:	
ICRF	20–28* MW
ECH	30* MW

* Upgrade.

a Oak Ridge National Laboratory, Oak Ridge, TN.
b New York University, New York, NY.
c Argonne National Laboratory, Argonne, IL
d McDonnell-Douglas Missile Systems Co., St. Louis, MO.
e Lawrence Livermore National Lab., Livermore, CA.
f Massachusetts Institute of Technology, Cambridge, MA.
g University of Wisconsin, Madison, WI.
h General Atomics, San Diego, CA.

iary heating power, and a fusion power of 110 MW. The energy confinement time is projected to be 0.93 s using ITER89–P scaling with an enhancement factor of only 1.42. A review of the available data on quasi-steady-state, relatively low q, H-mode performance leads one to conclude that enhancement factors in the range of 1.5–2.2 should be expected, with a median of 1.85.[2] The choice of 1.4 is thus a conservative one. The profiles are square-root parabolic for the density and trapezoidal (with a break point at r/a≈0.3) for the temperature. Thus, no benefit is taken for the enhanced reactivity expected with more peaked profiles, even though CIT will be equipped with a high-speed (4–5 km/s-) pellet injector and numerous techniques for recycling control. A Z_{eff} of 1.65 (from carbon and helium ash) is assumed, consistent with the experience in high-field Alcator tokamaks, which maintained low Z_{eff} at high density. The density ($\langle n_e \rangle = 1.5 \times 10^{20}$ m^{-3}) and beta (1.2%) needed to realize minimum performance are well within established operating limits: the density is about 20% of the Greenwald limit and the beta is about 25% of the Troyon limit. The temperature is about 9.2 keV.

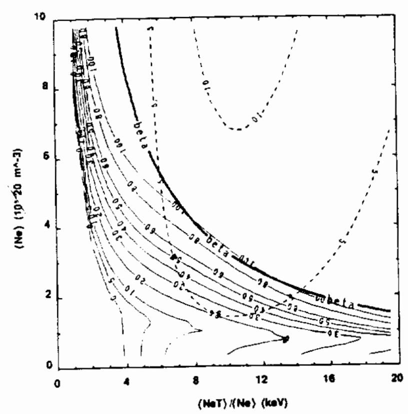

FIG. 1 CIT plasma operation contours (POPCON) for minimum-performance assumptions(τ_E=1.42xITER–P, 0.5% He). A conservative estimate of the beta limit, $\beta=2I_p/aB_T$, is used. With 20 MW of auxiliary heating, a fusion power of 100 MW and Q=5 is obtained, sufficient for burning-plasma physics studies. Solid contours: auxiliary power; dashed contours: Q.

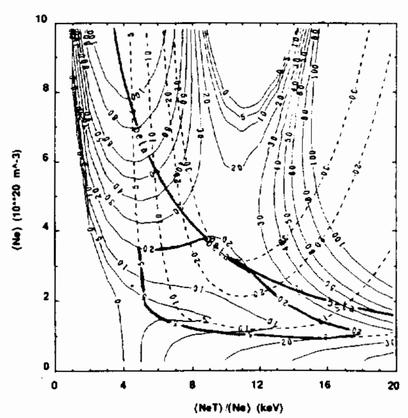

FIG. 2 POPCON for standard-performance assumptions (τ_E=1.85xITER–P). A fusion power of 500 MW is obtained at Q ≈ 27.

Standard performance projections suggest that CIT should significantly exceed the minimum requirements. With a confinement enhancement factor of 1.85 (the mean of the H–mode data), the plasma operating space is as shown in Figure 2. An energy gain of 27 and fusion power of 500 MW are obtained, still well within operating limits ($\langle n_e \rangle = 3.1 \times 10^{20}$ m^{-3}, β=3.0%). The energy confinement time is 0.82 s, lower than the minimum-performance case due to the higher power, and the temperature is 9.7 keV. This level of performance will permit the investigation of plasma behavior under conditions approaching ignition, where $P_\alpha >> P_{aux}$. Moreover, a wide burning-plasma operating space is available, bounded by Q=5, P_{aux}=20 MW, and the beta limit. Above-average confinement will enable CIT to reach beta values near the Troyon limit (5%), provided no lower stability limits intervene, to assess alpha effects on beta limits. The actual performance level will of course depend on plasma confinement, stability, and alpha heating efficiency, none of which can be predicted with certainty for burning plasmas. Indeed, the main objective of the CIT experiment is to determine these properties in order to gain the necessary predictive capability for ITER and future tokamaks.

Flexibility is an explicit requirement because of the uncertainty in predicting the optimum operating modes. Thus, CIT will have operating modes with double-null (DN) divertor, single-null (SN) divertor, inboard limiter, and "full-bore" plasma configurations. Fueling capabilities will include both 1.5 km/s and 4–5 km/s velocity pellets to allow density profile control. The baseline ICRF heating system will be tunable from 60 to 90 MHz. The device and facility can accommodate an ECH system as an upgrade for heating flexibility. Wall conditioning techniques will include beryllium evaporation and boron/carbon film deposition in addition to the high-power pulsed discharge cleaning and bakeout capabilities. The tokamak will provide at least 3,000 shots at maximum current and field; however, 30,000 shots will be available at two-thirds parameters for performance optimization and physics studies.

DISRUPTION ANALYSIS

Although the nominal CIT parameters lie within normally-stable operating boundaries, the possibility of major disruptions cannot realistically be excluded. Because of the high magnetic and thermal energy of the plasma, the loads imparted to the vacuum vessel, supports, and internal hardware are potentially quite severe when the plasma disrupts. The structural design of these components is therefore largely determined by disruption loads. Because it directly impacts the radial build of the tokamak, the most critical region is the inboard vacuum vessel wall, particularly the bolted joint between the modules. The vessel in that region is made of a high-strength alloy (Inconel 625) with a wall thickness of 7 cm.

To determine the disruption loads, time-dependent, axisymmetric simulations are performed using the Tokamak Simulation Code (TSC), which self-consistently models plasma equilibrium and the currents in the coils and structural components. The simulations include vertical and radial plasma motion and both toroidal and poloidal currents. In highly shaped tokamaks the fast vertical disruptions, or "Vertical Displacement Events (VDEs)" are particularly dangerous, having caused large structural loads on DIII–D, JET, and PBX–M. Examination of the magnetic data from such events has shown that substantial "halo" currents flow along open field lines in the plasma scrapeoff layer and into the vessel and internal components. The vessel provides a return path for these currents and the electromagnetic load distributions are significantly affected as a result. Since the halo currents pass through the first wall components, their electromagnetic loads are also altered. In the past year the TSC code has been modified to handle halo currents and has been calibrated against PBX–M.

Based on extrapolations from data, CIT disruptions are characterized by a thermal quench time of < 1 ms, a current quench rate of up to 3 MA/ms, and a poloidal halo current of 10–20% of the initial toroidal plasma current in VDEs. Experimentally, a VDE is precipitated by a loss of vertical control due to a change in profiles or a shift of the plasma to a region of unstable field curvature. (In TSC this is simulated by imposing an external field perturbation and disabling the feedback control system.) The plasma begins to drift vertically with little or no loss of current; as it does, the cross section shrinks, q decreases, and halo currents begin to flow. The halo region is characterized by a radial width corresponding to 40% of the plasma poloidal flux and a resistivity corresponding to an average plasma temperature of up to 20 eV. A force-free condition is imposed in this region, such that the current is parallel to the magnetic field everywhere. The current quench phase of the VDE is initiated when q_{95} reaches a critical value, about 2, which typically occurs 60 cm from the midplane. Measurements on DIII–D show poloidal halo currents during both the drift and the current-quench phases. The halo parameters in TSC are modeled on the basis of this behavior. Figure 3 displays the time history of the toroidal plasma and vacuum vessel currents, halo current, and the resulting electromagnetic pressure on the inboard vessel wall. The peak pressure in this case is about 35 atm. The distribution of forces during the current quench phase is shown in Figure 4. Interestingly, the presence of the halo currents slows the vertical drift and current quench rate in the simulations, in agreement with experiment. The halo temperature was reduced from 20 to 2 eV in the preceding example to pro-

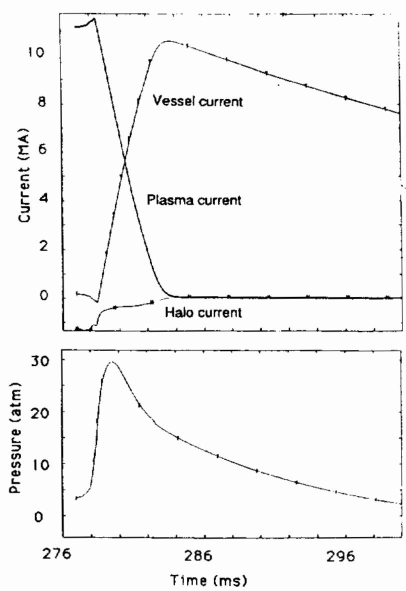

FIG. 3 a) Time histories of current during the disruption phase of a vertical displacement event. The disruption occurs ~ 60 cm below the midplane. The fast current decay (3 MA/ms) requires reduced halo temperatures during the disruption phase. b) Time history inboard vacuum vessel wall pressure.

duce a 3 MA/ms current decay. With a slightly higher temperature (4.5 eV) in the current decay phase, the decay rate is slower (0.5 MA/ms) and the halo current increases during the current decay phase. The effect of this on the vacuum vessel forces is being evaluated.

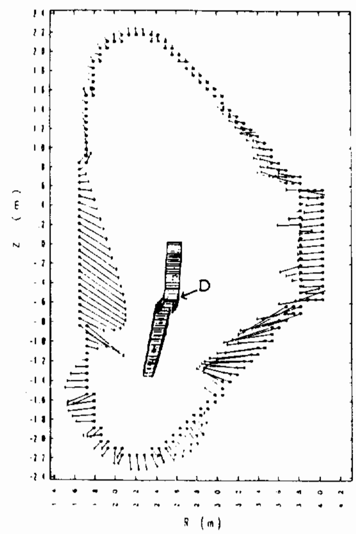

FIG. 4 Relative vacuum vessel force vectors (represented by the arrows) from TSC during the cur- rent quench phase of a VDE. Small squares indicate plasma trajectory from the start of drift (I_p=11.8 MA) to the time depicted (I_p=4.9 MA). The disruption point is indicated by "D".

POWER HANDLING

Under burning-plasma condition, up to 100 MW of thermal power (from alpha, auxiliary, and Ohmic heating) must be exhausted through the plasma surface area with an average power density of 1 MW/m^2. However, peak power densities are much higher where the separatrix strikes the divertor surface. To minimize the impact on plasma performance due to fuel dilution by impurities and due to bremsstrahlung radiation, low Z_{eff} ($\leq$ 1.65) must be maintained. This is reflected in the CIT design in the use of high plasma densities and low–Z first wall materials operated at a pre-shot temperature of 350^{o}C. The relatively short pulse length permits the use of inertial cooling with high-thermal-performance materials. Pyrolytic graphite is the material presently proposed for the divertor and carbon-carbon composites for the limiter.

In estimating the divertor heat fluxes, realistic divertor-channel imbalances are assumed: in DN divertor mode the up:down imbalance is 1.2:1, and the out:in imbalance is 4:1. Plasma energy losses are conservatively assumed to be 60% in charged particle flux to the divertor, 20% in bulk radiation, and 20% in edge radiation. The separatrices are swept poloidally across a ~ 20 cm wide area to maintain a surface temperature less than 1700^{o}C, since TFTR[3] shows sharp increases in carbon influx above temperatures in that range. With divertor sweeping, the temperature rise on the target surface is proportional to $P(\lambda_E FV)^{-0.5}$, where P is the power to the target, λ_E is the energy scrapeoff thickness at the outboard midplane, F is the flux expansion factor (about 10) and V is the sweep velocity. The scrapeoff layer is found to be not well characterized by exponentials, so λ_E represents only a characteristic width. Since P and F are given, λ_E and V are the critical parameters. At the outboard midplane, λ_E is calculated to be ~ 5 mm (so $\Lambda \approx$ 5 cm), based on 2D edge modeling with the Braams B2 code.[4] Nominal perpendicular diffusivities $D=\chi_i=1$ m^2/s and $\chi_e=3$ m^2/s are used, consistent with DIII–D experimental results[5].

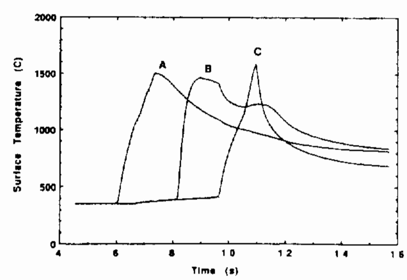

FIG. 5 Time histories of outboard divertor target surface temperature for ignited P_{fus}=500 MW discharge and swept divertor. Maximum accumulated peaking factorsare assumed. Traces correspond to points at thebeginning (A), middle (B), and end (C) of the sweep trajectory.

Divertor temperature calculations take into account the divertor sweep trajectory derived from TSC discharge simulations, the temperature-dependent properties of the pyrolytic graphite divertor plates, and the initial temperature of 350°C. A toroidal peak-to-average asymmetry of 1.5:1 is assumed, which will be maintained through careful control of field errors and tile alignment. The time-dependence of V is optimized to balance the heating across the plates. Using the specified physics guidelines, the divertor power handling capability permits a ~ 3.2–s burn at 500 MW of fusion power. The calculated temperature rise in the plates is shown in Figure 5. Estimates of the net erosion for these conditions, obtained using the REDEP[6] code, are <3000Å per shot, or <1 mm for the life of the machine. Even with a conservative estimate of the temperature at the divertor (65 eV), net erosion is limited because of: 1)the short pulse length, 2)divertor sweeping, and 3)the high calculated densities (7×10^{20} m^{-3}) in the vicinity of the plates.

The physics models and assumptions for the edge plasma are continually being upgraded. Further work will be done under the CIT Physics R&D program.

ICRF HEATING

The baseline auxiliary heating system for CIT will be fast-wave ICRF at a power level of 20 MW and a pulse length of 15 s. This is sufficient to heat the plasma to standard-performance conditions (P_{fus}=500 MW, Q≈30) within the available time. The ICRF frequency will be tunable over the range 60–90 MHz to permit ^{3}He minority heating from 2/3 to full magnetic field (6–9 T). The heating resonance will change to second-harmonic tritium as the plasma beta increases. The 20 MW of ICRF power will be coupled through four two-strap loop antennas. The current strap elements (two per strap) and transmission line feeds (two per element) will be installed through and supported by the large outboard ports. The Faraday shields will be installed from the interior of the vacuum vessel and mounted on the vessel wall. The present design utilizes mechanically attached graphite tiles on the shields, but alternatives such as beryllium tiles are also being evaluated.

The antenna arrangement, shown in plan view in Figure 6, provides a total radiating area of 0.6 m^2 (0.6 m x 1.0 m) per antenna, for a required power density of 8.6 MW/m^2. This compares with power densities of 10 MW/m^2 recently achieved in TFTR limiter discharges[7]; however, the power density in JET H–mode discharges (with an external separatrix) is limited to ~3 MW/m^2. The expected power density limit due to transmission-line breakdown in the CIT antennas corresponds to about 24 MW/m^2, so power handling limits may be determined by antenna-plasma interactions. The antenna and Faraday shield designs are therefore being optimized to minimize breakdown and impurity generation on the shield. The shield elements will be slanted parallel to the local magnetic field and 0–π phasing of the current straps will be used. Information obtained through continued theoretical and experimental research will lead to a better understanding of the mechanisms that limit power handling and will be used to optimize the CIT antenna design. Such research is an important component of the CIT Physics R&D Plan.

Load resistance (R_L) calculations for the CIT antenna have recently begun using a 2D recessed antenna model. The model treats an antenna of infinite length in a slab geometry, but treats the scrapeoff plasma, antenna cavity, and strap geometry in a realistic manner and gives good agreement with TFTR data. The resistance is sensitive to the scrapeoff density profile, which is uncertain. For an assumed separatrix density of 1.5×10^{20} m^{-3} and e–folding width of 1 cm, R_L varies from 5 to 10 Ω as the antenna-separatrix spacing is varied from 6 to 2 cm. This provides ample loading for the power densities required and suggests that plasma separatrix position (along with small frequency shifts) can be used to dynamically tune the load impedance to match through the L–H transition. Such a technique has been successfully demonstrated on JET.[8] Further research in the area of ICRF heating with H–mode is an important R&D need for CIT. Experiments at high density and magnetic field are especially desirable.

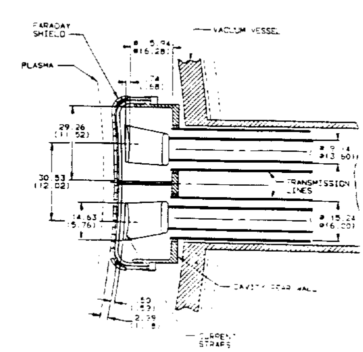

FIG. 6 Plan view of ICRF antenna.

DIAGNOSTICS

The CIT will require a substantial complement of specialized diagnostics to carry out its mission. The set will include diagnostics to investigate the alpha population and related phenomena, such as the source rate, fast and slow alpha particle densities, fast alpha energy distribution, alpha-driven instabilities, and alpha losses. It will also include diagnostics to make the range of plasma measurements found on existing devices, including profiles of electron density, ion and electron temperature, and radiation; impurity content; fluctuations over a range of scale lengths; edge and divertor properties; and plasma configuration.

Some new diagnostic techniques must be developed to meet CIT requirements. Candidate alpha-particle diagnostic methods include far-infrared laser scattering, microwave scattering at high gyrofrequency harmonics, and detection of gammas from nuclear reactions between alphas and injected impurities. Even for some of the more "traditional" measurements, new methods are needed because of the harsh environment. The magnetic loops are especially vulnerable because they are subjected to both high temperatures (~ 1200°C) and high radiation fluxes (1.5×10^{18} n/m^2/s). Thus, measurements of the effects of radiation on insulators (as well as on windows and detectors) are needed. While fluence effects on long-term damage are well known, more data are needed on flux-related effects such as radiation-induced absorption and fluorescence, changes in conductivity, and signal degradation due to nuclear heating. Component development needs include improved laser and gyrotron sources and radiation-hardened bolometer detectors. Conceptual design studies have been conducted for selected diagnostics, which has provided an opportunity to begin to address some of the more difficult diagnostic systems and many of the generic diagnostic issues.

CONCLUSIONS

The basic machine parameters of CIT will provide the high plasma performance needed to accomplish its burning-plasma mission. This is achieved through an engineering approach that follows the Alcator line of high-performance tokamaks. Vacuum vessel and divertor loads are partly determined by plasma physics phenomena, which are analyzed in detail for the CIT design. Plasma heating and diagnostic systems must operate under demanding conditions. Nevertheless, credible design concepts have been developed and an R&D plan has been formulated to acquire the additional data needed to optimize the design.

ACKNOWLEDGEMENT

This work was supported by the U. S. Department of Energy under Contract No. DE–AC02–76–CHO3073.

REFERENCES

[1] D. J. Sigmar et al., "Physics Objectives and Design of CIT," paper IAEA-CN-53/G–1–1 presented at 13th Int. Conf. on Plasma Physics and Controlled Nuclear Fusion Research, Washington, 1–6 October, 1990.

[2] R. J. Goldston et al., "A Physics Perspective on CIT," Proc. 17th EPS Conf. on Controlled Fusion and Plasma Heating, Amsterdam, 25–29 June 1990, paper I–134.

[3] M. Ulrickson, paper presented at the 9th Int. Conf. on Plasma Surface Interactions, Bournemouth, UK, May, 1990; to be published in J. Nucl. Mat.

[4] B.J. Braams and C.E. Singer, Fusion Technology **9**, (1986) 320.

[5] D.N. Hill, et al. GA-A20138 (1990) to be published in J. Nucl. Mater.

[6] J. N. Brooks, J. Nucl. Mat. **170** (1990) 164–168.